A Method of Using Nonidentical Resonant Coils for Frequency Splitting Elimination in Wireless Power Transfer

Yue-Long Lyu, *Student Member, IEEE*, Fan-Yi Meng, *Member, IEEE*, Guo-Hui Yang, *Member, IEEE*, Bang-Jun Che, Qun Wu, *Senior Member, IEEE*, Li Sun, *Member, IEEE*, Daniel Erni, *Member, IEEE*, and Joshua Le-Wei Li, *Fellow, IEEE*

***Abstract*—In this paper, an efficient method is proposed to eliminate frequency splitting in nonradiative wireless power transfer via magnetic resonance coupling. In this method, two nonidentical resonant coils (NIRCs) are used as wireless power transmitter and receiver, respectively. According to the elliptic integral term in the analytical expression, the pole of the mutual inductance function with respect to transfer distance can be eliminated by using the two NIRCs, and hence overcoupling between transmitter and receiver with close transfer distance is avoided. Therefore, frequency splitting caused by overcoupling can be suppressed and stable output power can be achieved. The NIRCs are analytically calculated, numerically simulated and finally, fabricated and tested to verify the theory. All the calculated and experimental results show that frequency splitting is completely eliminated and uniform voltage across the load is achieved. Furthermore, lateral misalignment between the NIRCs barely introduces frequency splitting, and the suppression level of frequency splitting can also be controlled freely.**

***Index Terms*—Frequency splitting, magnetic resonance coupling, nonidentical resonant coils (NRCs), wireless power transfer (WPT).**

I. Introduction

WIRELESS power transfer via magnetic resonance coupling (WPT/MRC) has been a research hotspot during recent years since the inspiring work of A. Kurs *et al*. was reported in *Science* in 2007 [1]–[7]. It is pointed out that magnetic resonant coils in the WPT/MRC system can wirelessly exchange electromagnetic (EM) power efficiently by magnetic coupling, and the transfer distance is much longer compared with the conventional WPT via inductive coupling [8]–[10]. Therefore, such WPT/MRC can be widely applied in portable consumer electronic, medical, and industrial devices such as charging vehicles, endoscopes, laptops and so on [11]–[15]. In general, for both the WPT via inductive coupling and the WPT/MRC, the power received by the target increases as the transmitting coil gets close to the receiving coil. However, for a WPT/MRC system, once the distance between the transmitting and receiving coils is smaller than a threshold value, the received power drops sharply because of the magnetic overcoupling between the transmitting and receiving coils. In this case, the received power reaches its peak value not at the original resonant frequency but at two adjacent frequencies, and thus, this phenomenon is called as frequency splitting [11], [16]–[18]. Consequently, WPT/MRC operating at a fixed frequency suffers dramatically changed received power when transmitting and receiving coils move relatively to each other [19]. The research on frequency splitting, in cooperation with other technologies such as the power capability enhancement technology [20], [21], undoubtedly contributes to broadening the applications of WPT/MRC, which currently mainly aims at midrange power transfer.

Frequency splitting has been analyzed first based on coupling mode theory [22]. Then a few circuit models are established to explain and describe frequency splitting [11], [23]–[25]. As essentially caused by the nonuniform magnetic field distribution of the resonant coil, frequency splitting widely exists in WPT/MRC systems. To obtain uniform received power with respect to transfer distance against frequency splitting, several methods have been presented. In [11], a WPT/MRC transmitter consisting of two coils referred as drive loop and transmitting coil, respectively, was proposed, and frequency splitting can be suppressed by simultaneously adjusting the EM coupling strength between the drive loop and transmitting coil according to transfer distance of the WPT/MRC system. The control of EM coupling is usually achieved by mechanically adjusting the relative position or attitude of the drive loop and the transmitting coil. However, such adjustment is difficult to implement for mobile receivers because in this case, people have to constantly shift the relative position to resist frequency splitting [11], [19],

Manuscript received August 22, 2014; revised November 11, 2014; accepted December 23, 2014. Date of publication January 6, 2015; date of current version July 10, 2015. This work was supported in part by the Open Project Program of the State Key Laboratory of Millimeter Wave under Grant K201403. *(Corresponding author: F.-Y. Meng.)* Recommended for publication by Associate Editor A. Covic.

Y.-L. Lyu, G.-H. Yang, B.-J. Che, and Q. Wu are with the Department of Microwave Engineering, Harbin Institute of Technology, Harbin 150001, China (e-mail: lvyuelonglvyuelong@126.com; gh.yang@hit.edu.cn; chebangjun1991@163.com; qwu@hit.edu.cn).

F.-Y. Meng is with the Department of Microwave Engineering, Harbin Institute of Technology, Harbin 150001, China, and also with the State Key Laboratory of Millimeter Waves, Nanjing 210096, China (e-mail: blade@hit.edu.cn).

L. Sun is with the School of Electrical Engineering and Automation and with the Department of Electrical Engineering, Harbin Institute of Technology, Harbin 150001, China (e-mail: motor611@sina.com).

D. Erni is with the Laboratory for General and Theoretical Electrical Engineering (ATE), Faculty of Engineering, and the Center for Nanointegration Duisburg-Essen (CENIDE), University of Duisburg-Essen, D-47048 Duisburg, Germany (e-mail: daniel.erni@uni-due.de).

J. L.-W. Li is with the Institute of Electromagnetics and School of Electronic Engineering, University of Electronic Science and Technology of China, Chengdu 611731, China, with the Advanced Engineering Platform and School of Engineering, Monash University, Selangor 46150, Malaysia, and also with the Department of Electrical and Computer Systems Engineering, Monash University, Melbourne, Vic. 3800, Australia (e-mail: joshua.li@monash.edu).

Color versions of one or more of the figures in this paper are available online at http://ieeexplore.ieee.org.

Digital Object Identifier 10.1109/TPEL.2014.2387835

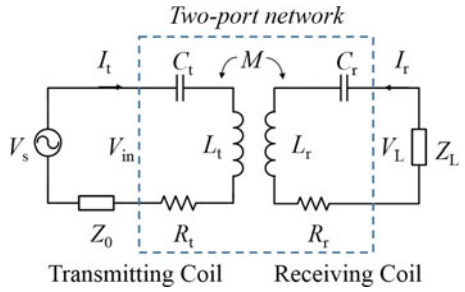

Fig. 1. Equivalent circuit model of two-loop WPT system.

[24], [26]. Frequency tracking is another solution to effectively transfer EM power in strong coupling region. The WPT/MRC system implementing this method transfers EM power not at the fixed resonant frequency but at a varying optimal frequency, and hence, a series of complex control circuits are required in the WPT/MRC system, such as differential amplifier, phase compensator, phase-locked loop and so on [11], [19], [27], [28], which occupy specialized space and introduce additional power consumption. Lee *et al.* [29] uses tunable impedance matching network to extend the range of the available transfer distance in both weak and strong coupling regions, but the network also needs control circuit to switch corresponding impedance matching channel according to the transfer distance. In addition, improved structures of resonant coils are also proposed for frequency splitting suppression [30], [31]. In 2013, Lee *et al.* proposed antiparallel resonant loops to offset the excess mutual inductance to avoid frequency splitting [31]. However, the antiparallel loops further weaken the mutual inductance in weak coupling region and consequently, the maximum transfer distance of the WPT/MRC system is shortened.

In this paper, a method adopting a pair of nonidentical transmitting and receiving coils is proposed to eliminate frequency splitting and obtain uniform received power for WPT. Analytical calculations, numerical simulations, and experimental measurements show that such nonidentical resonant coils (NIRCs) can be properly designed to eliminate the magnetic overcoupling between the transmitter and receiver. Consequently, frequency splitting is eliminated without complex additional control circuit and simultaneous impedance matching. The transfer coefficient of the system is uniform regardless of the transfer distance in the work range.

II. Theory Description

A. Equivalent Circuit Model of WPT/MRC

A common WPT/MRC system consists of two resonant coils: A transmitting coil and a receiving coil. The equivalent circuit model can be described as shown in Fig. 1. Both the transmitting coil and the receiving coil can be considered as series loops composing of capacitance (C_t, C_r), inductance (L_t, L_r), and copper wire resistance (R_t, R_r) of the resonant coils. The port characteristic impedance of the transmitting coil is R_0, and the load impedance of the receiving coil is R_L. The mutual inductance *M* is introduced to describe the magnetic coupling between the two coils. The resonant frequency f_0 of the WPT/MRC system can be denoted by

$$\omega_0 = \frac{1}{\sqrt{L_t C_t}} = \frac{1}{\sqrt{L_r C_r}} = 2\pi f_0. \tag{1}$$

In order to simplify the calculation and derivation, the two coils are assumed lossless ($R_t = R_r = 0$), because R_t and R_r (usually less than 5 Ω, different from the case of WPT via inductive coupling where the coil resistance cannot be ignored due to the large turn number [8, 32]) are much smaller than R_0 and R_L (e.g., both 50 Ω in this paper). The following experiment in this paper shows that this approximation barely affects the transfer characteristics analysis. This is because, for a WPT/MRC system, the reduction of the power received by the load mainly depends on the mismatch, neither the radiation nor Ohm loss in the coils. The relationship between currents through either coil and the voltage across either port can be expressed as the following Z matrix (impedance matrix) (2) through applying Kirchhoff's voltage law to this system, which can be viewed as a two-port network [see Fig. 1]

$$\begin{pmatrix} V_{\text{in}} \\ V_L \end{pmatrix} = \begin{pmatrix} j\omega L_t + \dfrac{1}{j\omega C_t} & j\omega M \\ j\omega M & j\omega L_r + \dfrac{1}{j\omega C_r} \end{pmatrix} \begin{pmatrix} I_t \\ I_r \end{pmatrix} \tag{2}$$

where V_{in} is the voltage across the input port of the transmitting coil, and V_L is the voltage across the output port of the receiving coil, i.e., the voltage across R_L. The relationship among V_L, V_{in}, and the source voltage V_s [see Fig. 1] can be established by (3), where R_0 and R_L are both resistive

$$S_{21} = \frac{V_L/\sqrt{R_L} - I_r\sqrt{R_L}}{V_{\text{in}}/\sqrt{R_0} + I_t\sqrt{R_0}} = \frac{2V_L}{V_s}\sqrt{\frac{R_0}{R_L}}. \tag{3}$$

Therefore, the power transfer property of the system could be described by transfer coefficient, S_{21}, which is very convenient to be obtained experimentally by vector network analyzer (VNA) [11]. In WPT/MRC system with constant source voltage V_s, S_{21} can be directly used to estimate the power received by the load because V_L is proportional to S_{21} according to (3). For analytical calculation, S_{21} can be derived as (4) from matrix (2) using the classic conversion formulas given in [33]

$$S_{21} = \frac{2j\omega M\sqrt{R_0 R_L}}{M^2\omega^2 + \left(\omega L_t - \dfrac{1}{\omega C_t} + R_0\right)\left(\omega L_r - \dfrac{1}{\omega C_r} + R_L\right)}. \tag{4}$$

When the WPT/MRC system operates at f_0, S_{21} can be simplified as

$$S_{21} = \frac{2}{\dfrac{\omega_0 M}{\sqrt{R_0 R_L}} + \dfrac{\sqrt{R_0 R_L}}{\omega_0 M}} \tag{5}$$

and S_{21} reaches up to its maximum value (1 in ideal model ignoring radiation loss and heat loss in coils) when the mutual inductance *M* equals to M_m as

$$M_m = \frac{\sqrt{R_0 R_L}}{\omega_0}. \tag{6}$$

According to (5) and (6), S_{21} decreases as M goes far away from M_m. Especially when M is larger than M_m, the transmitter and receiver work in strong coupling region where the transmitter and receiver is close to each other, and S_{21} drops rapidly with frequency splitting occurring.

B. Method for Frequency Splitting Elimination

As mentioned above, frequency splitting is caused by the magnetic overcoupling between the transmitter and the receiver. Therefore, the investigation of frequency splitting and its suppression should begin with the analytical analysis of the mutual inductance. For the simplest case, both the receiver and the transmitter of the WPT/MRC system are single-turn circular resonant coils whose radiuses are r_1 and r_2, respectively, and are placed face-to-face with a distance d. The mutual inductance M can be calculated through the function $M(d)$ defined as (7) [34]

$$\begin{cases} M(d) = \mu_0 \dfrac{\sqrt{r_1 r_2}}{g}\left[\left(2-g^2\right)K\left(g^2\right) - 2E\left(g^2\right)\right] \\ g^2 = \dfrac{4r_1 r_2}{d^2 + (r_1 + r_2)^2} \end{cases} \tag{7}$$

where $K(^*)$ and $E(^*)$ are the complete elliptic integrals of the first and second kind, respectively. In the general WPT system, transmitting coil and receiving coil have the same or similar dimensions [1], [11], [35]. Especially for the case where transmitting and receiving coils are identical $(r_1 = r_2)$, g rapidly approaches 1 as the receiving coil moves close to the transmitting coil, that is, $d \to 0$. Because $K(1) = \infty$ and $E(1) = 1$, $M(d)$ increases rapidly with the decrease of the d between the two coils. As a result, the optimum transfer consideration is destroyed and frequency splitting occurs.

Therefore, the key point of the frequency splitting elimination is maintaining g much less than 1 for any distance to avoid the pole, $K(1) = \infty$. By keeping in mind this principle and mathematically analyzing (7), one can find that unequal r_1 and r_2 leads to g less than 1 for any distance, with which the pole of $M(d)$ disappears. As a result, the curve of $M(d)$ versus d becomes flat, and frequency splitting can be eliminated once M gets close with M_m in a large distance range.

In order to validate the above prediction, a series of M values are calculated and depicted in Fig. 2 under the condition of $r_1 \neq r_2$, where r_1 equals to a set value of 3 cm and r_2 varies in a large range. A curve of the case $r_2 = r_1 = 3$ cm is also depicted in Fig. 2 as a reference [blue lines in both Fig. 2(a) and (b)]. A sharp rise of this curve with d tending to be 0 indicates the pole of $M(d)$ at $d = 0$. This dramatic change leads to a small distance range where M closes to M_m, only in which the S_{21} maintains large value according to (5).

The calculated M values are divided into two groups as shown in Fig. 2(a) and (b), respectively. The curves depicted in Fig. 2(a) present $M(d)$ for the case of $r_1 > r_2$, and those in (b) for the case of $r_1 < r_2$. For the both cases, all the curves of $M(d)$ increases with the decrease of d, but the growth slows down as the difference between r_1 and r_2 increases, which means the effect of the pole of $M(d)$ is gradually weakened. The pole can be completely eliminated if the radius difference is large enough according to Fig. 2(a) and (b). Especially for the case of $r_1 < r_2$, as shown in Fig. 2(b), not only M with close distance suppressed, but also that with long distance is enhanced due to the strong magnetic field excited by the large transmitting coil, whereas the M for the case of $r_1 > r_2$ is small at long distance because the magnetic field excited by small transmitting coil is not strong. This indicates that transmitter with large size is suitable in the practice system for frequency suppression and it will be discussed in the following section.

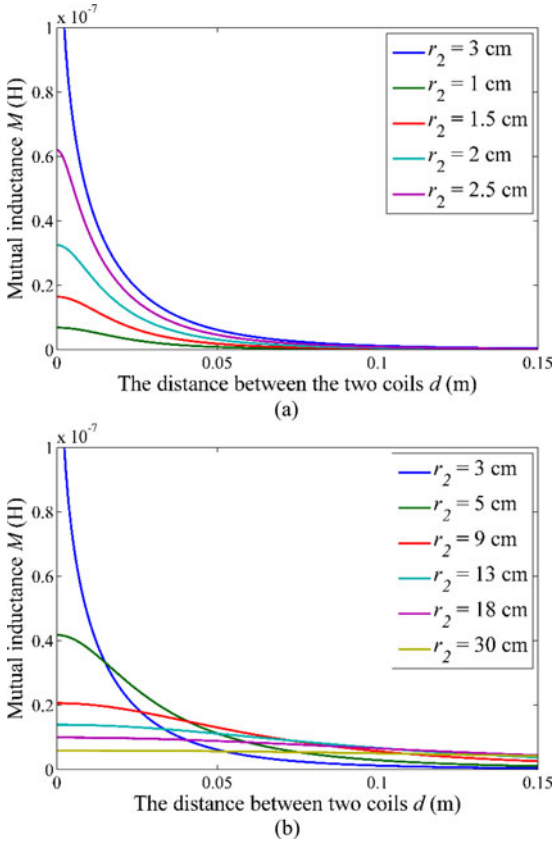

Fig. 2. Mutual inductance with respect to transfer distance between two circular coils with different radius, where (a) is $r_2 < r_1$ and (b) is $r_2 > r_1$.

C. Analytical Calculation of S_{21} of the WPT/MRC System With Frequency Suppression and Elimination

To analyze the effect of the curve flatness of $M(d)$ on transfer characteristics of the WPT/MRC system, a series of S_{21} of WPT/MRC systems adopting different pairs of transmitter and receiver are calculated through (4) and depicted in Fig. 3(a)–(f). The parameter description of these pairs of transmitter and receiver are listed in Table I. The inductance in Table I can be calculated through (8) [34]

$$L_n = \mu_0 r_n \left[\log\left(\frac{8r_n}{a}\right) - 1.75\right],\ n = 1, 2 \tag{8}$$

where a is the wire radius. The capacitance C_n contains the self-capacitance of the coil and series capacitor. The turn number n_1 and n_2 of the coils mainly depend on the optimal mutual

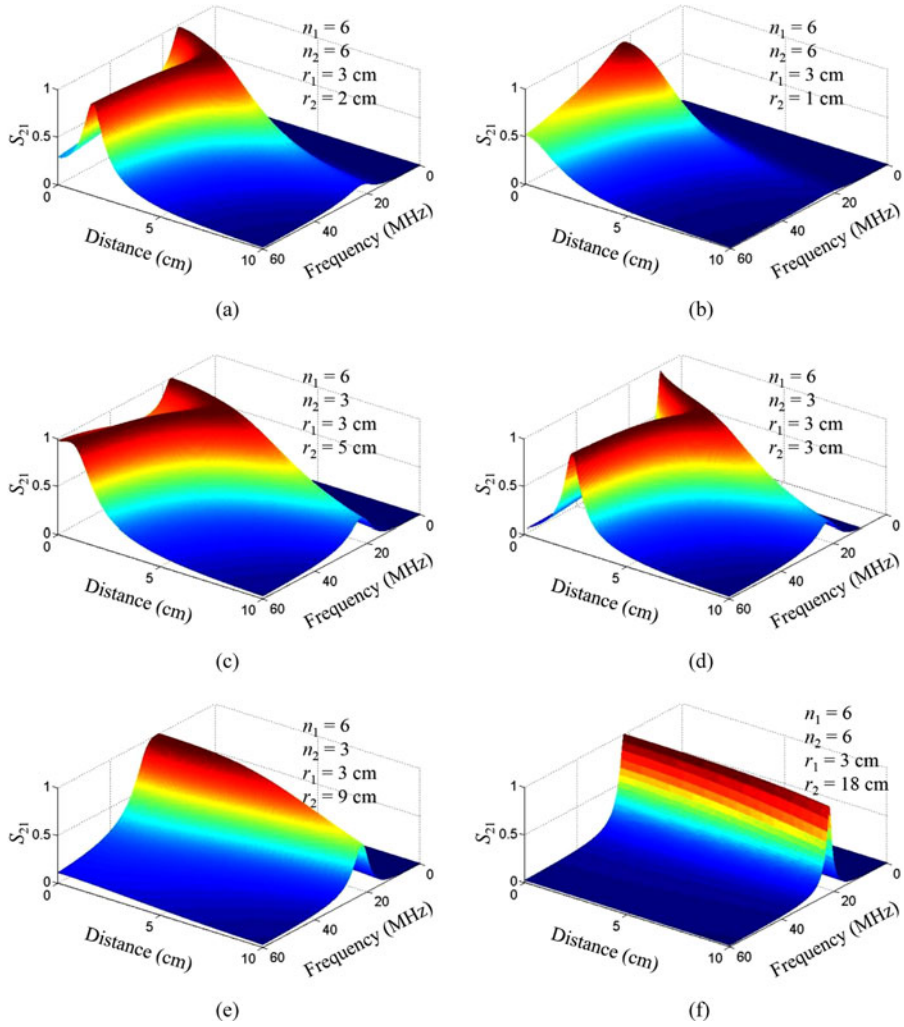

Fig. 3. Transfer coefficient S_{21} between transmitting and receiving coils with different parameters.

TABLE I
PARAMETERS OF RESONANT COILS FOR THEORY ANALYSIS

	Receiving Coil	Transmitting Coil
Radius	$r_1 = 3$ cm	r_2
Number of turns	$n_1 = 6$	n_2
Inductance	L_1	L_2
Series capacitor	C_1	C_2
Resonant frequency	$f_0 = 22.1$ MHz	
Wire radius	$a = 1$ mm	

inductance M_m defined by (6) as

$$n_1 n_2 M(d) = M_m . \tag{9}$$

The parameter values for the six cases shown in Fig. 3 are listed in the corresponding subfigures, respectively.

Similar to the analysis in the last section, the S_{21} for the case of $r_1 = r_2 = 3$ cm is investigated first and plotted in Fig. 3(c) as a reference. From Fig. 3(c), one can observe obvious frequency splitting phenomenon that the maximum S_{21} peak splits into two peaks as the transfer distance decays. For the case of $r_1 = 3$ cm and $r_2 = 2$ cm, the region where frequency splitting occurs is compressed but the transfer distance is also shortened as shown in Fig. 3(b). As r_2 decreases further, such as the case of $r_2 = 1$ cm shown in Fig. 3(a), frequency splitting can be eliminated completely but the maximum transfer distance is shortened further.

From Fig. 3(d) to (f), one can find that frequency splitting is suppressed gradually with the increase of r_2. In Fig. 3(d), the two peaks of the S_{21} in frequency splitting region are much closer compared with the case shown in (c), and the valley between the two peaks is also shallower than that in (c). When the radius difference is large enough, such as cases shown in (e) and (f), frequency splitting is completely eliminated, and the S_{21} peak becomes flatter as the radius of the transmitter is larger.

The fluctuation of all the S_{21} curves versus transfer distance at the original resonant frequency f_0 in Fig. 3 shows good consistence with the variation trend of $M(d)$ curves depicted in Fig. 2. The steeper the $M(d)$ curve is, the more dramatically the S_{21} declines in strong coupling region where frequency splitting occurs, and the flatter the $M(d)$ curve is, the more uniform the

S_{21} versus transfer distance is. Compared with the S_{21} depicted in Fig. 3(e), one can find that the S_{21} in (f) is more uniform and maintains large value in a broader distance range. One should note that in the case of (f), the coil turn is increased to make up the weakened magnetic field according to (9) to meet the consideration (6).

From Fig. 3, one can conclude that a relatively large transmitter to receiver is suitable to be adopted in the WPT/MRC system to eliminated frequency splitting and achieve uniform S_{21} in a large distance range. Compared with the method proposed in [31], the maximum transfer distance can be extended because the large transmitter adopted in this method enhances the magnetic field at long distance instead of offsetting it as reported in [31]. Designers only need to think about the tradeoff between the uniformity of S_{21} and the size of the transmitter. In fact, the size of the receiver attracts more consideration than that of the transmitter because the size of the device to be charged is usually strictly restricted by the application environment such as endoscope [12] but the size of transmitter is usually not restricted that strictly [26]. Therefore, the method proposed in this paper can be a good alternative of that in [31] and [36], in the case where there is no strict restriction on the size of the transmitter. In addition, the proposed method does not require extra control mechanism such as simultaneous impedance matching and frequency splitting, which makes it easy to design and apply.

What is worth noting that the proposed method for frequency splitting elimination is universal for coils of other shapes as well, such as rectangle resonant coils. The key point is to eliminate the pole of $M(d)$ and this can be achieved by properly adjusting the relative sizes of transmitter and receiver through the corresponding calculation expression, for example, M of regular coils can be calculated through the expressions in [31], [36], and [37]. For coils of complicated shapes, between which M cannot be calculated easily or precisely, numerical simulation can be implemented to calculate M and optimize the coil sizes for frequency splitting suppression and elimination.

III. Numerical Simulation and Experimental Results

According to the analytical calculation, the pairs of resonant coils of the sizes listed in Fig. 3(e) and (f) shows good frequency splitting elimination performance. Considering the tradeoff between transfer characteristics and the sizes of the resonant coils, a pair of NIRCs are designed based on the parameters of the case shown in Fig. 3(e) and modeled in HFSS, a commercial software package based on finite-element method, as illustrated in Fig. 4. As the calculation in Section II is ideal, the parameters of the simulated NIRCs are slightly modified for simulation convenience and precision.

As shown in Fig. 4, the transmitting coil is three-turn copper wire with wire width $w = 1$ mm. The largest radius is $r_2 = 9.25$ cm. The gap between adjacent loops is $g = 1$ mm. The small resonant coil is six-turn copper wire with the largest radius $r_1 = 3.25$ cm. The rest of its parameters are the same as the large resonant coil. Both of the two coils are connected with capacitors in series to resonate at 17.5 MHz. The coils shown in Fig. 4 are also fabricated using enameled wires with series

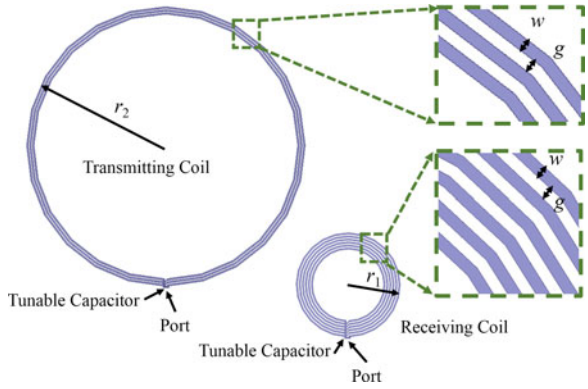

Fig. 4. Structures and parameters of the NIRCs for frequency splitting elimination, where $r_1 = 3.25$ cm, $r_2 = 9.25$ cm, and $w = g = 1$ mm.

Fig. 5. Prototype of NIRCs.

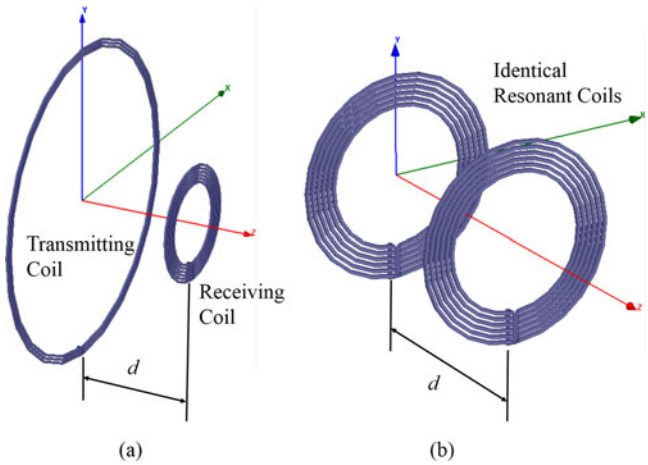

Fig. 6. Simulation models in HFSS, where (a) is the NIRCs and (b) is the IRCs.

tunable capacitors as shown in Fig. 5. Limited by fabrication procedure, deviation between the fabricated and ideal coils cannot be avoided, but this deviation has no serious impacts on the performance of WPT/MRC according to the measured results.

The NIRCs are placed face-to-face as shown in Fig. 6(a). The distance between the NIRCs is d, varying from 0 to 7 cm. A pair of identical resonant coils (IRCs), shown in Fig. 6(b) is also simulated and experimentally tested corresponding to the case shown in Fig. 3(c) as reference, and hence, they are the same as the receiving coil in the pair of the NIRCs.

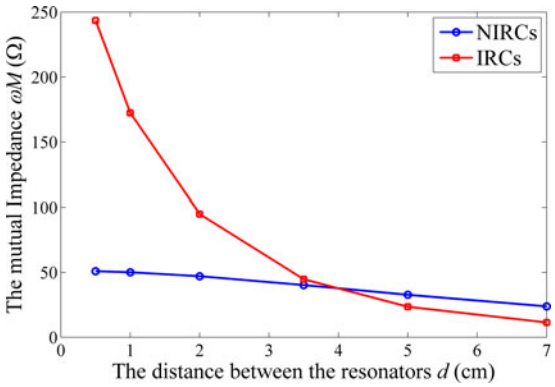

Fig. 7. Imaginary part of the mutual impedance between two resonators versus distance at 17.5 MHz.

In the numerical simulation, ωM can be directly got as it is the imaginary part of the mutual impedance between the transmitting and receiving coil. The simulated ωM for the both cases at 17.5 MHz is simulated and depicted in Fig. 7. The curve of the IRCs changes dramatically as the distance between the coils decreases, which agrees with $M(d)$ depicted in Fig. 2. As R_0 and R_L are set 50 Ω, the optimal ωM value should also be 50 Ω for maximum power transfer according to (6). Therefore, frequency splitting occurs because of the overcoupling at close distance, and S_{21} also decays at long distance due to the weak coupling. On the contrary, ωM of the NIRCs maintains around 50 Ω and S_{21} can be predicted to stay at the peak value without frequency splitting at both close transfer distance and long distance.

Both the transfer coefficient S_{21} of systems using NIRCs and IRCs are simulated and then, measured by VNA, Agilent N5227A. As shown in Figs. 8 and 9, both the simulated and measured S_{21} agree with each other very well. The S_{21} of NIRCs stays at peak value near 0 dB at the resonant frequency 17.5 MHz with different transfer distance, and no frequency splitting is observed. On the other hand, the S_{21} of the IRCs stays at 0 dB at 17.5 MHz only with $d = 3.5$ cm. Frequency splitting occurs and reduces S_{21} at the resonant frequency as d decreases. Both the results depicted in Figs. 8 and 9 show good consistence with those in Fig. 3(c) and (e), respectively. The tendency and magnitude of the S_{21} for the both cases validate the proposed theory reliably.

To clearly observe the results of both the NIRCs and IRCs, the S_{21} with respect to transfer distance at resonant frequency for the both cases are depicted in Fig. 10. There exists a reduction about 2 dB between the peak values of the simulated results and the measured ones. The reduction can be caused by fabrication deviation, loss in components, radiation, and port and experiment operation errors. From Fig. 10, one can observe that the S_{21} of the NIRCs is much more uniform than that of IRCs and the value maintains at high level. The S_{21} is enhanced by 6.5 dB in the original strong coupling region.

Practical WPT/MRC systems are also established using the pairs of NIRCs and IRCs. Agilent E8257D is used as signal generator and is connected with a power amplifier (PA). The PA is connected with the large resonant coil, and the small resonant coil is connected with a load. The waveforms in this WPT/MRC

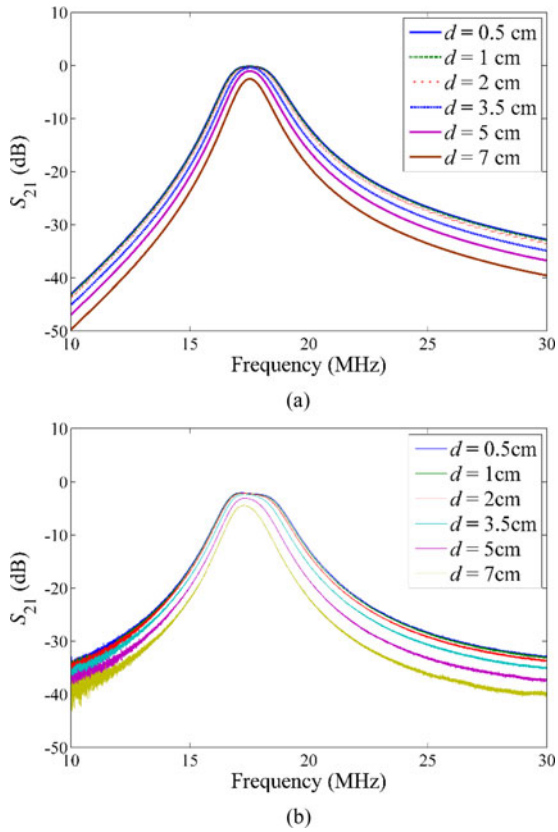

Fig. 8. Transfer coefficient S_{21} of the NIRCs with different transfer distance, where (a) shows the simulated results and (b) shows the measured results.

system are measured by Lecroy Wave Master 8600A. The measured results of WPT/MRC with IRCs and NIRCs at the resonant frequency are shown in Figs. 11 and 12, respectively.

The waveforms (a) in both Figs. 11 and 12 are the output voltage of the PA when directly connected with a 50-Ω load, whereas the waveforms (b), (c), and (d) in both Figs. 11 and 12 are the voltage across the 50-Ω load connected with the receiving coil as the receiving coil moves away from the transmitting coil. According to Figs. 11 and 12, there is no waveform distortions but amplitude variation between the transmitter and the receiver. The amplitude of the output waveform of the WPT/MRC system with IRCs (shown in Fig. 11) varies dramatically, whereas the amplitude of the output waveform of the WPT/MRC system with NIRCs keeps large value and varies slightly as shown in Fig. 12. The two series of sinusoidal waveforms verify the proposed method in the time domain.

LEDs are also implemented as the load in WPT/MRC to intuitively reflect the transfer characteristic of WPT/MRC, as shown in Fig. 13. The LEDs of WPT/MRC using IRCs becomes dim whether the transfer distance is too close or too long, whereas the LED brightness of WPT/MRC using NIRCs keeps strong in the same whole region. All the experimental results reflect in all aspects that frequency splitting in WPT/MRC can be effectively eliminated and large and flat transfer coefficient can be easily obtained. Different from the results shown in Figs. 8–10, the results shown in Figs. 11–13 directly verify the proposed theory by the realized power received by the load.

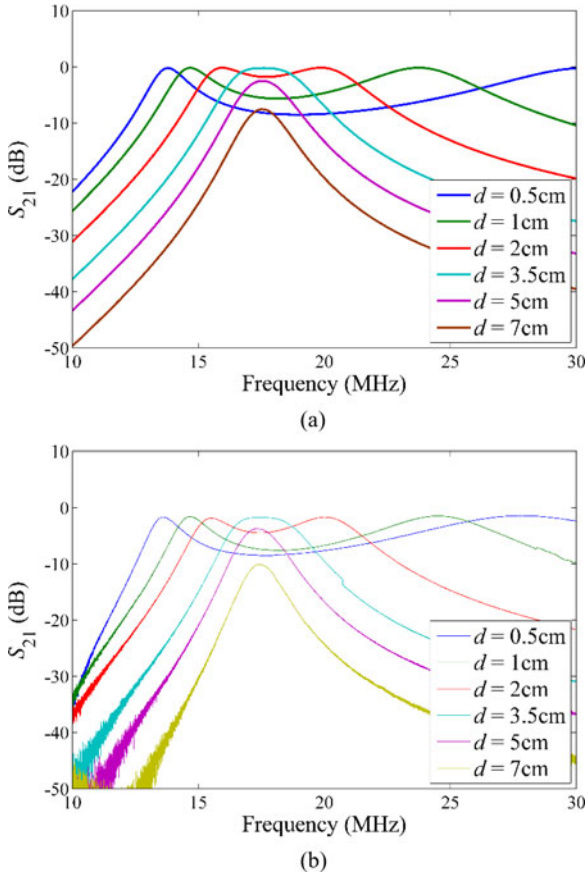

Fig. 9. Transfer coefficient S_{21} of the IRCs with different transfer distance, where (a) shows the simulated results and (b) shows the measured results.

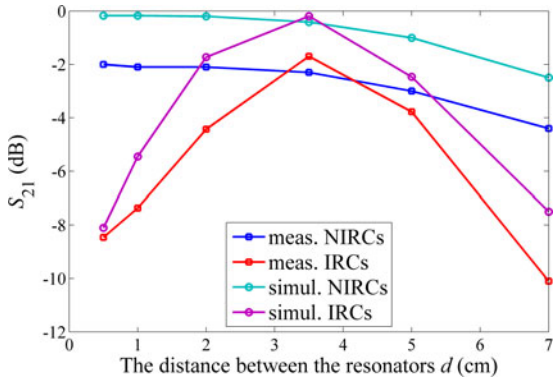

Fig. 10. Transfer coefficient S_{21} contrast between the NIRCs and the IRCs at 17.5 MHz.

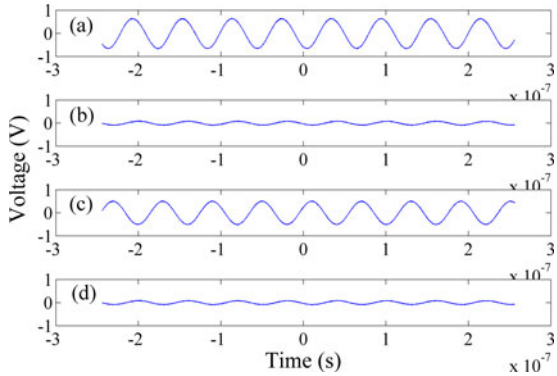

Fig. 11. Waveforms in WPT/MRC with IRCs, where (a) is the output voltage of the PA, and (b), (c), and (d) are the voltage across the load as the receiver moves away from the transmitter.

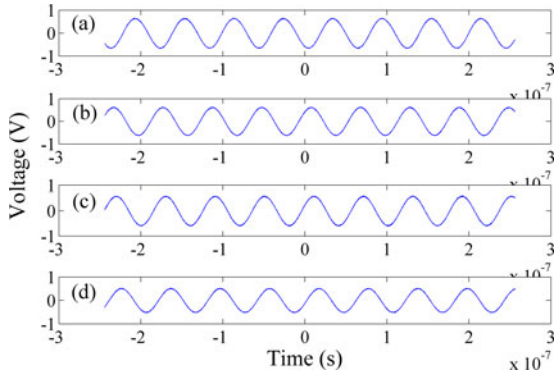

Fig. 12. Waveforms in WPT/MRC with NIRCs, where (a) is the output voltage of the PA, and (b), (c), and (d) are the voltage across the load as the receiver moves away from the transmitter.

IV. Discussion

A. Impact of the Lateral Misalignment of the NIRCs

The method proposed in this paper aims at the uniform transfer property with respect to transfer distance. Therefore, all the results above illustrate the performance of NIRCs with the same axis. It is also important to investigate the S_{21} for the case where there exists lateral misalignment when the NIRCs moves relatively as shown in Fig. 14 [38], [39]. The lateral misalignment along x-direction is defined as d_{x}. Fig. 15 illustrates the simulated results of the S_{21} of NIRCs (simulation model in Section III) taking lateral misalignment into consideration. In Fig. 15, the results of S_{21} with $d = 1$ cm and d_{x} varying from 0 to 7 cm are depicted. Only the curves of the case of $d_{\mathrm{x}} = 6$ and 7 cm show slight frequency splitting because the magnetic field near the edge of the transmitting coil is strong resulting excess coupling. Out of this region, there is no frequency splitting regardless of the position of the receiving coil relative to the transmitting coil due to the uniform magnetic field excited by the transmitting coil. Therefore, the charging region of the receiver with uniform transfer property is very large. In addition, the uniform transfer property could be further improved through clever design of the structure of the transmitting coil [40].

B. Estimation of Maximum Transfer Distance of WPT/MRC With NIRCs

Although the results shown in Section III illustrate that uniform transfer coefficient can be achieved in a large distance range by using NIRCs, one should note that the results do not mean NIRCs effectively contributes to extend the maximum transfer distance because the experiments in Section III are on the base that the dimension of the receiver is constant. IRCs

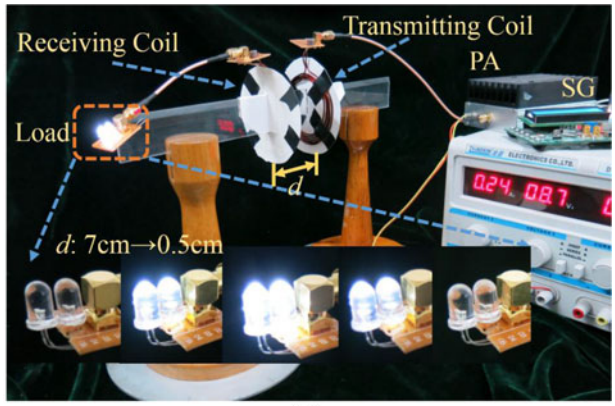

(a)

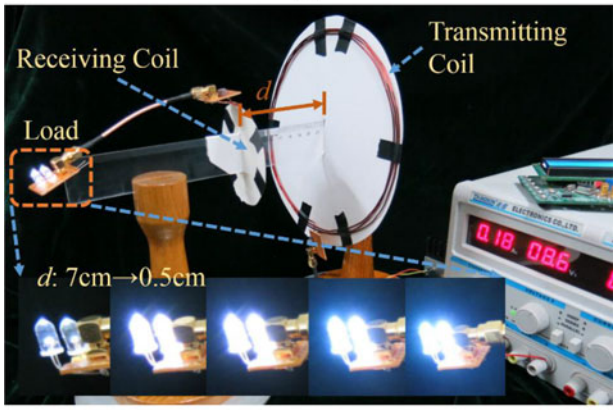

(b)

Fig. 13. Practical WPT/MRC system with (a) IRCs and (b) NIRCs using LED as load, respectively.

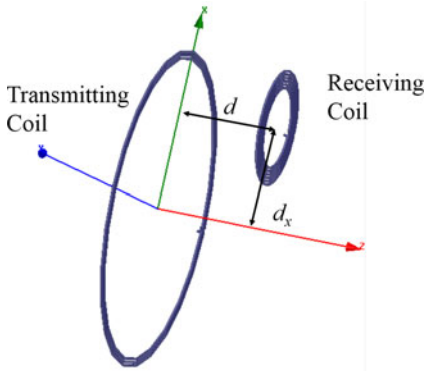

Fig. 14. NIRCs with lateral misalignment.

with equivalent radius defined by (10) should be introduced as reference to estimate the maximum transfer distance of the WPT/MRC system using NIRCs

$$r_{\mathrm{eq}} = \frac{r_1 + r_2}{2}. \tag{10}$$

A comparison of S_{21} at resonant frequency is conducted between WPT/MRC using NIRCs and IRCs with equivalent radius, and the results are shown in Fig. 16.

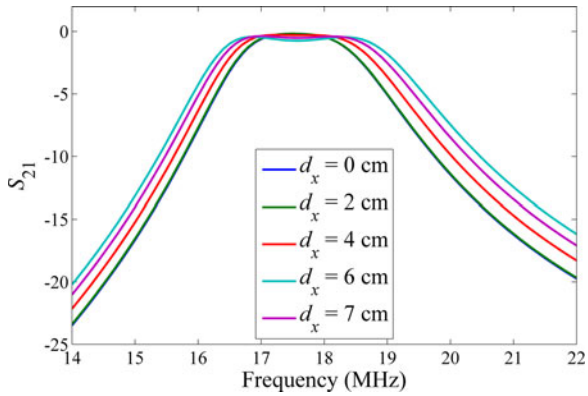

Fig. 15. Simulated S_{21} taking lateral misalignment into consideration.

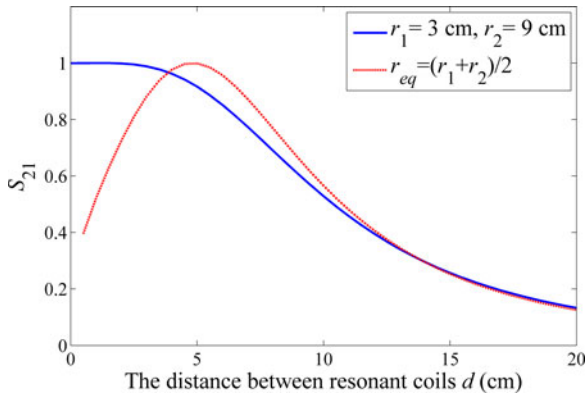

Fig. 16. Transfer coefficient S_{21} comparison between the WPT/MRC system using NIRCs and IRCs with equivalent radius.

From Fig. 16, one can find that system using IRCs with equivalent radius shows better performance at long transfer distance than system using NIRCs, but the difference between the two curves at long distance is small. Therefore, using NIRCs achieves uniform S_{21} in large distance range with limited decrease of the maximum transfer distance of the WPT/MRC system.

C. Level Control of Frequency Splitting Suppression

In the experiments in Section III, frequency splitting is totally eliminated. Actually, the suppression level of frequency splitting can be controlled by adjusting the relative dimension of the NIRCs. In this section, S_{21} of systems, operating at resonant frequency and using four pairs of NIRCs, are analytically calculated and depicted in Fig. 17. The key parameters of these cases are listed in Table II. The equivalent radius of the four pairs of NIRCs are the same so that the maximum power transfer regions of the four cases have overlap for clear comparison. According to Fig. 17, the suppression level of frequency splitting can be freely controlled by reasonably adjusting the difference between the sizes of the transmitter and receiver. One could design the relative dimensions of the NIRCs according to the available charging range of the receiver in practice.

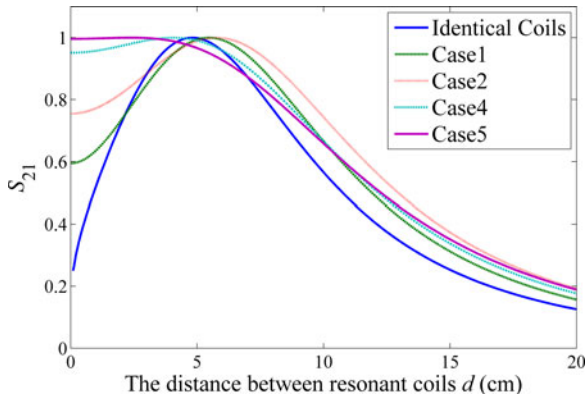

Fig. 17. Transfer coefficient S_{21} comparison between the WPT/MRC system using different NIRCs with the same equivalent radius.

TABLE II
PARAMETERS OF RESONANT COILS FOR THE COMPARISON OF THE LEVEL CONTROL OF FREQUENCY SPLITTING

	Radius	Number of turns
IRCs	$r_1 = r_2 = r_{eq} = 6$ cm	$n_1 = n_2 = 3$
Case 1	$r_1 = 5$ cm, $r_2 = 7$ cm	$n_1 = 4, n_2 = 3$
Case 2	$r_1 = 4$ cm, $r_2 = 8$ cm	$n_1 = 6, n_2 = 3$
Case 3	$r_1 = 3$ cm, $r_2 = 9$ cm	$n_1 = 6, n_2 = 4$
Case 4	$r_1 = 2$ cm, $r_2 = 10$ cm	$n_1 = 7, n_2 = 7$

V. CONCLUSION

In this paper, a pair of nonidentical transmitting and receiving coils is proposed as an approach to avoid the magnetic over-coupling in WPT/MRC. Therefore, frequency splitting can be suppressed or completely eliminated, and uniform output power can be achieved. Analytical calculation, numerical simulation, and experiment are conducted and results agree with each other. The proposed NIRCs present an effective approach to cope with frequency splitting without extra control mechanism, which is easy to design and apply in practice.

ACKNOWLEDGMENT

The authors would like to thank Prof. Y.-J. Feng and Prof. X.-Y. Zhang for very fruitful discussions. The authors would also like to thank Dr. S. Lin, H. Liu, and Y.-Q. Zhao for helping conduct the experiments.

REFERENCES

[1] A. Kurs, A. Karalis, R. Moffatt, J. D. Joannopoulos, P. Fisher, and M. Soljačić, "Wireless power transfer via strongly coupled magnetic resonances," *Science*, vol. 317, no. 5834, pp. 83–86, 2007.
[2] N. Shinohara, "Power without wires," *IEEE Microw. Mag.*, vol. 12, no. 7, pp. S64–S73, Dec. 2011.
[3] E. Waffenschmidt, "Wireless power for mobile devices," in *Proc. IEEE 33rd Int. Telecommun. Energy Conf.*, 2011, pp. 1–9.
[4] C. Kainan and Z. Zhengming, "Analysis of the double-layer printed spiral coil for wireless power transfer," *IEEE J. Emerging Sel. Topics Power Electron.*, vol. 1, no. 2, pp. 114–121, Jun. 2013.
[5] N. Wai Man, Z. Cheng, L. Deyan, and S. Y. R. Hui, "Two- and three-dimensional omnidirectional wireless power transfer," *IEEE Trans. Power Electron.*, vol. 29, no. 9, pp. 4470–4474, Sep. 2014.
[6] S. Y. R. Hui, Z. Wenxing, and C. K. Lee, "A critical review of recent progress in mid-range wireless power transfer," *IEEE Trans. Power Electron.*, vol. 29, no. 9, pp. 4500–4511, Sep. 2014.
[7] B.-J. Che, G.-H. Yang, F.-Y. Meng, K. Zhang, J.-H. Fu, Q. Wu, and L. Sun, "Omnidirectional non-radiative wireless power transfer with rotating magnetic field and efficiency improvement by metamaterial," *Appl. Phys. A, Mater. Sci. Process.*, vol. 116, no. 4, pp. 1579–1586, Sep. 2014.
[8] M. Budhia, J. T. Boys, G. A. Covic, and C. Y. Huang, "Development of a single-sided flux magnetic coupler for electric vehicle IPT charging systems," *IEEE Trans. Ind. Electron.*, vol. 60, no. 1, pp. 318–328, Jan. 2013.
[9] F. van der Pijl, P. Bauer, and M. Castilla, "Control method for wireless inductive energy transfer systems with relatively large air gap," *IEEE Trans. Ind. Electron.*, vol. 60, no. 1, pp. 382–390, Jan. 2013.
[10] D. Kurschner, C. Rathge, and U. Jumar, "Design methodology for high efficient inductive power transfer systems with high coil positioning flexibility," *IEEE Trans. Ind. Electron.*, vol. 60, no. 1, pp. 372–381, Jan. 2013.
[11] A. P. Sample, D. A. Meyer, and J. R. Smith, "Analysis, experimental results, and range adaptation of magnetically coupled resonators for wireless power transfer," *IEEE Trans. Ind. Electron.*, vol. 58, no. 2, pp. 544–554, Feb. 2011.
[12] A. K. RamRakhyani and G. Lazzi, "On the design of efficient multi-coil telemetry system for biomedical implants," *IEEE Trans. Biomed. Circuits Syst.*, vol. 7, no. 1, pp. 11–23, Feb. 2013.
[13] C. S. Wang, O. H. Stielau, and G. A. Covic, "Design considerations for a contactless electric vehicle battery charger," *IEEE Trans. Ind. Electron.*, vol. 52, no. 5, pp. 1308–1314, Oct. 2005.
[14] P. T. Theilmann and P. M. Asbeck, "An analytical model for inductively coupled implantable biomedical devices with ferrite rods," *IEEE Trans. Biomed. Circuits Syst.*, vol. 3, no. 1, pp. 43–52, Feb. 2009.
[15] J. Sallan, J. L. Villa, A. Llombart, and J. F. Sanz, "Optimal design of ICPT systems applied to electric vehicle battery charge," *IEEE Trans. Ind. Electron.*, vol. 56, no. 6, pp. 2140–2149, Jun. 2009.
[16] L. H. Chen, S. Liu, Y. C. Zhou, and T. J. Cui, "An optimizable circuit structure for high-efficiency wireless power transfer," *IEEE Trans. Ind. Electron.*, vol. 60, no. 1, pp. 339–349, Jan. 2013.
[17] B. L. Cannon, J. F. Hoburg, D. D. Stancil, and S. C. Goldstein, "Magnetic resonant coupling as a potential means for wireless power transfer to multiple small receivers," *IEEE Trans. Power Electron.*, vol. 24, no. 7, pp. 1819–1825, Jul. 2009.
[18] Y. Kim and H. Ling, "Investigation of coupled mode behaviour of electrically small meander antennas," *Electron. Lett.*, vol. 43, no. 23, pp. 1250–1252, 2007.
[19] P. Jongmin, T. Youndo, K. Yoongoo, K. Youngwook, and N. Sangwook, "Investigation of adaptive matching methods for near-field wireless power transfer," *IEEE Trans. Antennas Propag.*, vol. 59, no. 5, pp. 1769–1773, May 2011.
[20] L. Seung-Hwan and R. D. Lorenz, "Development and validation of model for 95%-efficiency 220-W wireless power transfer over a 30-cm air gap," *IEEE Trans. Ind. Appl.*, vol. 47, no. 6, pp. 2495–2504, Nov./Dec. 2011.
[21] S.-H. Lee and R. D. Lorenz, "Surface spiral coil design methodologies for high efficiency, high power, low flux density, large air-gap wireless power transfer systems," in *Proc. IEEE 28th Annu. Appl. Power Electron. Conf. Expo.*, 2013, pp. 1783–1790.
[22] A. Karalis, J. D. Joannopoulos, and M. Soljacic, "Efficient wireless non-radiative mid-range energy transfer," *Ann. Phys.*, vol. 323, no. 1, pp. 34–48, Jan. 2008.
[23] Y. Zhang and Z. Zhao, "Frequency splitting analysis of two-coil resonant wireless power transfer," *IEEE Antennas Wireless Propag. Lett.*, vol. 13, pp. 400–402, Mar. 2014.
[24] Y. Zhang, Z. Zhao, and K. Chen, "Frequency splitting analysis of four-coil resonant wireless power transfer," *IEEE Trans. Ind. Appl.*, vol. 50, no. 4, pp. —2436–2445, Jul./Aug. 2013.
[25] J. Y. Lan, H. J. Tang, and X. Gen, "Frequency splitting analysis of wireless power transfer system based on T-type transformer model," *Elektronika Ir Elektrotechnika*, vol. 19, no. 10, pp. 109–113, 2013.
[26] H. Hoang, S. Lee, Y. Kim, Y. Choi, and F. Bien, "An adaptive technique to improve wireless power transfer for consumer electronics," *IEEE Trans. Consum. Electron.*, vol. 58, no. 2, pp. 327–332, May 2012.
[27] W. Q. Niu, J. X. Chu, W. Gu, and A. D. Shen, "Exact analysis of frequency splitting phenomena of contactless power transfer systems," *IEEE Trans. Circuits Syst. I, Reg. Papers*, vol. 60, no. 6, pp. 1670–1677, Jun. 2013.
[28] K. Nam Yoon, K. Ki Young, R. Young-Ho, C. Jinsung, K. Dong-Zo, Y. Changwook, P. Yun-Kwon, and K. Sangwook, "Automated adaptive frequency tracking system for efficient mid-range wireless power transfer via magnetic resonanc coupling," in *Proc. 42nd Eur. Microw. Conf.*, 2012, pp. 221–224.
[29] W. S. Lee, H. L. Lee, K. S. Oh, and J. W. Yu, "Switchable distance-based impedance matching networks for a tunable HF system," *Prog. Electromagn. Res.*, vol. 128, pp. 19–34, 2012.

[30] M. Ettorre and A. Grbic, "A transponder-based, nonradiative wireless power transfer," *IEEE Antennas Wireless Propag. Lett.*, vol. 11, pp. 1150–1153, Oct. 2012.
[31] W. S. Lee, W. I. Son, K. S. Oh, and J. W. Yu, "Contactless energy transfer systems using antiparallel resonant loops," *IEEE Trans. Ind. Electron.*, vol. 60, no. 1, pp. 350–359, Jan. 2013.
[32] Y. Zhang, Z. Zhao, and K. Chen, "Frequency decrease analysis of resonant wireless power transfer," *IEEE Trans. Power Electron.*, vol. 29, no. 3, pp. 1058–1063, Mar. 2014.
[33] D. A. Frickey, "Conversions between S, Z, Y, H, ABCD, and T parameters which are valid for complex source and load impedances," *IEEE Trans. Microw. Theory Tech.*, vol. 42, no. 2, pp. 205–211, Feb. 1994.
[34] A. Grbic, R. Merlin, E. M. Thomas, and M. F. Imani, "Near-field plates: Metamaterial surfaces/arrays for subwavelength focusing and probing," *Proc. IEEE*, vol. 99, no. 10, pp. 1806–1815, Oct. 2011.
[35] C. K. Lee, W. Zhong, and S. Hui, "Effects of magnetic coupling of nonadjacent resonators on wireless power domino-resonator systems," *IEEE Trans. Power Electron.*, vol. 27, no. 4, pp. 1905–1916, Apr. 2012.
[36] S. Raju, R. X. Wu, M. S. Chan, and C. P. Yue, "Modeling of mutual coupling between planar inductors in wireless power applications," *IEEE Trans. Power Electron.*, vol. 29, no. 1, pp. 481–490, Jan. 2014.
[37] W. G. Hurley and M. C. Duffy, "Calculation of self and mutual impedances in planar magnetic structures," *IEEE Trans. Magn.*, vol. 31, no. 4, pp. 2416–2422, Jul. 1995.
[38] K. Fotopoulou and B. W. Flynn, "Wireless power transfer in loosely coupled links: Coil misalignment model," *IEEE Trans. Magn.*, vol. 47, no. 2, pp. 416–430, Feb. 2011.
[39] S. Aldhaher, P. C. K. Luk, and J. F. Whidborne, "Electronic tuning of misaligned coils in wireless power transfer systems," *IEEE Trans. Power Electron.*, vol. 29, no. 11, pp. 5975–5982, Nov. 2014.
[40] J. Kim, H. C. Son, and Y. J. Park, "Multi-loop coil supporting uniform mutual inductances for free-positioning WPT," *Electron. Lett.*, vol. 49, no. 6, pp. 417–419, 2013.

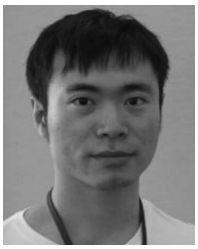

Yue-Long Lyu (S'14) received the B. E. and M. E. degrees in microwave engineering from the Harbin Institute of Technology (HIT), Harbin, China, in 2012 and 2014, respectively, where he is currently working toward the Ph.D. degree in the Department of Microwave Engineering

His current research interests include wireless power transfer and tunable microwave device and antenna.

Mr. Lyu received the Student Travel Award from the IEEE International Conference on Microwave Magnetics in July 2014, Sendai, Japan, and the Student Paper Contest Award (honorable prize) from the 3rd IEEE Asia-Pacific Conference on Antennas and Propagation, July 2014, Harbin, China.

Fan-Yi Meng (S'07–M'09) received the B.S., M.S., and Ph.D. degrees in electromagnetics from the Harbin Institute of Technology, Harbin, China in 2002, 2004, and 2007, respectively.

Since August 2007, he has been with the Department of Microwave Engineering, Harbin Institute of Technology, where he is currently a Professor. He has coauthored four books, 40 international refereed journal papers, more than 20 regional refereed journal papers, and 20 international conference papers. His current research interests include antennas, electromagnetic and optical metamaterials, plasmonics, and electromagnetic compatibility.

Dr. Meng received several awards including the 2013 Top Young Innovative Talents of the Harbin Institute of Technology, the 2013 CST University Publication Award, the 2010 Award of Science and Technology from the Heilongjiang Province Government of China, the 2010 "Microsoft Cup" IEEE China Student Paper Contest Award, the two Best Paper Awards from the National Conference on Microwave and Millimeter Wave in China in 2009 and 2007, respectively, the 2008 University Excellent Teacher Award of the National University of Singapore, the 2007 Excellent Graduate Award of the Heilongjiang Province of China, and the Outstanding Doctor Degree Dissertation Award of the Harbin Institute of Technology.

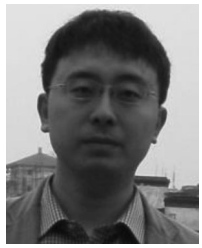

Guo-Hui Yang (S'07–M'09) received the B.S. degree in telecommunication, the M.S. degree in instrument science and technology, and the Ph.D. degree in electromagnetics all from the Harbin Institute of Technology, Harbin, China in 2003, 2006, and 2009, respectively.

Since 2009, he has been with the Department of Microwave Engineering, Harbin Institute of Technology, where he is currently an Associate Professor. His current research interests include RF MEMS device, tunable antenna, FSS, EMC, and FDTD.

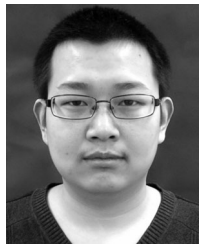

Bang-Jun Che received the B. E. and M. E. degrees in microwave engineering from the Harbin Institute of Technology (HIT), Harbin, China, in 2012 and 2014, respectively, where he is currently working toward the Ph.D. degree in the Department of Microwave Engineering.

His current research interests include wireless power transfer and tunable microwave device and antenna.

Mr. Che received the Student Paper Contest Award (second prize) from the 3rd IEEE Asia-Pacific Conference on Antennas and Propagation in July 2014, Harbin, China.

Qun Wu (M'93–SM'05) received the B.Sc. degree in radio engineering, the M.Eng. degree in electromagnetic fields and microwaves, and the Ph.D. degree in communication and information systems from the Harbin Institute of Technology (HIT), Harbin, China, in 1977, 1988, and 1999, respectively.

He was a Visiting Professor with Seoul National University, Seoul, Korea, from 1998 to 1999, and with the Pohang University of Science and Technology, from 1999 to 2000. He was a Visiting Professor with the National University of Singapore, from 2003 to 2010. Since 1990, he has been with the School of Electronics and Information Engineering, HIT, where he is currently a Professor and the Head of the Department of Microwave Engineering. He is also the Director of the Center for Microwaves and EMC. He published several books and more than 100 international and regional refereed journal papers. His recent research interests mainly include electromagnetic compatibility, metamaterials, and antennas.

Prof. Wu received the Science and Technology Award from Heilongjiang Provincial Government in 2010. He is a Member of the Microwave Society of the Chinese Institute of Electronics. He is a Technical Reviewer for several international journals. He is also the Vice Chair of the IEEE Harbin Section, and the Chair of IEEE Harbin EMC/AP/MTT Joint Society Chapter. He was the Chair or a Member in the TPC of international conferences for many times. He is also invited to give a keynote report or invited papers in some international conferences for many times.

Li Sun (M'08) was born in Heilongjiang Province, China, in 1960. He received the B.S., M.S., and Ph.D. degrees in electrical engineering from the Harbin Institute of Technology, Harbin, China, in 1982, 1986, and 1991, respectively.

Since 1986, he has been with the Department of Electrical Engineering, Harbin Institute of Technology, where he is currently a Professor in electrical machine and apparatus. His research interests include the fields of electric machines and drives, renewable energy, power electronics and their applications, and EMC.

Daniel Erni (S'88–M'93) received the Diploma degree in electrical engineering from the University of Applied Sciences, Rapperswil, Switzerland, in 1986, and the Diploma degree in electrical engineering and the Ph.D. degree from ETH Zürich, Zürich, Switzerland, in 1990 and 1996, respectively.

He was the Founder, and from 1995 to 2006, the Head of the Communication Photonics Group, ETH Zürich. Since 1990, he has been with the Laboratory for Electromagnetic Fields and Microwave Electronics, ETH Zürich. Since October 2006, he has been a Full Professor of general and theoretical electrical engineering at the University of Duisburg-Essen, Duisburg, Germany. His current research includes advanced data transmission schemes (i.e., O-MIMO) in board-level optical interconnects, optical on-chip interconnects, ultradense integrated optics, nanophotonics, plasmonics, quantum optics, and optical and electromagnetic metamaterials. The latter with a distinct emphasis on biomedical engineering, namely for advanced RF excitation schemes in magnetic resonance imaging. On the system level, he has pioneered the introduction of numerical structural optimization into dense integrated optics device design. Further research interests include science and technology studies as well as the history and philosophy of science with a distinct focus on the epistemology in engineering sciences.

Dr. Erni is a Member of the Editorial Board of the *Journal of Computational and Theoretical Nanoscience*. He is a Fellow of the Electromagnetics Academy. He is a Member of the Center for Nanointegration Duisburg-Essen. He is also as a Member of and the Applied Computational Electromagnetics Society, the Swiss Physical Society, the German Physical Society (DPG), and the Optical Society of America (OSA). He is an Associated Member of the Swiss Electromagnetics Research Centre.

Joshua Le-Wei Li (S'91–M'92–SM'96–F'05) received the B.Sc. degree in physics from Xuzhou Normal College, Xuzhou, China, in 1984, the M.Eng.Sc. degree in electrical engineering from the China Research Institute of Radiowave Propagation, Xinxiang, China, in 1987, and the Ph.D. degree in electrical engineering from Monash University, Melbourne, Australia, in 1992, respectively.

He was selected in 2009 by Chinese 1000-Talent Scheme (Qian-Ren Ji-Hua) as a QRJH Chair (National) Professor at the University of Electronic Science and Technology of China (UESTC) where he was appointed as the Founding Director of the Institute of Electromagnetics, the Director of the Centre for Space Polar Energy Microwave Power Transmission, and also the Vice Chairman of University Academic Committee, all from UESTC. He is currently a Professor of electrical and computer systems engineering in the School of Engineering at Monash University. His current research interests include electromagnetic theory (e.g., dyadic Green's functions), computational electromagnetics (e.g., precorrected fast Fourier transform method and adaptive integral method), radio wave propagation and scattering in various media (e.g., chiral media, anisotropic media, bianisotropic media, and metamaterials), microwave propagation and scattering in tropical environment, and analysis and design of various antennas (e.g., loop and wire antennas and microstrip antennas). In these areas, he has (co-)authored four books, 48 book chapters, more than 370 international refereed journal papers, 49 regional refereed journal papers, and more than 400 international conference papers.

Prof. Li received many awards from the IEEE, the Chinese Institute of Communications, the Chinese Institute of Electronics, National University of Singapore, UESTC, Monash University and so on. He also serves as a Member of various International Advisory Committee and/or Technical Program Committee of many international conferences or workshops.